*Polym. Sci. Polym. Phys. Ed.* **22**, 1085 (1984).
19. J. D. Hoffman, G. T. Davis, J. I. Lauritzen, in *Treatise on Solid State Chemistry*, N. B. Hannay, Ed. (Plenum, New York, 1976), vol. 3, chap. 7.
20. R. A. Chivers *et al.*, *J. Polym. Sci. Polym. Phys. Ed.* **20**, 1717 (1982).
21. Such results on polyethylene oxides are usually regarded as singularities in the polymer field rather than indicative of general behavior, particularly since other compounds, such as iodine-terminated polyethylenes of comparable polydispersity, did not display the quantized layer thickness effect (*9*). Nevertheless, a preference for chain ends to lie within the layer surface has been inferred even there, and also in short-chain polyethylenes with broad molecular-weight distributions [D. M. Sadler and A. Keller, *Kolloid Z. Z. Polym.* **242**, 1081 (1970)]. Our observations on *n*-alkanes are the more remarkable because the methyl end groups are closely similar to the chain members themselves. Nevertheless, the creation of vacancies when the methyl end groups are within the lattice or when they protrude from the layer appears sufficient to influence the fold length in the manner observed.
22. S. J. Spells and D. M. Sadler, *Polymer* **25**, 739 (1984).
23. S. J. Spells, A. Keller, D. M. Sadler, *ibid.*, p. 749.
24. S. J. Spells, *Polym. Commun.* **25**, 162 (1984).
25. G. V. Fraser, *Ind. J. Pure Appl. Phys.* **16**, 344 (1978).
26. We are indebted to P. Hendra for placing his Raman spectroscopic facility at our disposal when our own was not operational. G.U. and I.B. thank the Science and Engineering Research Council for financial support in the form of a research assistantship and a Ph.D. studentship, respectively.

26 December 1984; accepted 24 May 1985

# Amino Acid Replacements That Compensate for a Large Polypeptide Deletion in an Enzyme

Abstract. *Deletion of more than 400 amino acids from the carboxyl terminus of an enzyme causes a severe reduction in catalytic activity. Selected point mutations within the residual protein partially reverse the effects of the missing segment. The selection can yield mutants with activities at least ten times as high as those of the starting polypeptides. One well-characterized mutation, a single amino acid replacement in the residual polypeptide, increases the catalytic activity of the polypeptide by a factor of 5. The results suggest substantial potential for design of protein elements to compensate for missing polypeptide sequences. They also may reflect that progenitors of large aminoacyl-tRNA (transfer RNA) synthetases—one of which was used in these studies—were themselves much smaller.*

CALVIN HO
MARIA JASIN
PAUL SCHIMMEL
*Department of Biology, Massachusetts Institute of Technology, Cambridge 02139*

We examined the possibility that a substantially truncated protein can reacquire, through substitution of one or more amino acids some of the activity that is lost when a large polypeptide sequence is removed. Because there is no opportunity for compensatory interactions between mutant amino acids in the residual protein and the missing polypeptide sequences, the possibilities for restructuring the enzyme are limited.

There were two reasons for doing these studies. First, protein engineering is conceptually simpler and technically easier with small polypeptide chains. Many enzymes are large and, if they are to be redesigned or modified, the smallest possible unit of structure that retains activity is to be preferred. Removal of polypeptide sequences, however, can severely attenuate, if not eliminate, activity. This may pose constraints on how small an efficient enzyme for a particular reaction can be made.

The other reason concerns the overall design and organization of a particular class of enzymes, one member of which was investigated in these studies. These are the aminoacyl-tRNA (transfer RNA) synthetases (*1, 2*). Some of these enzymes are large polypeptides (approximately 1000 amino acids), but there are data that support the hypothesis that the progenitors of these large enzymes were themselves much smaller (*3, 4*). The question is whether a barely active, small subfragment of a large synthetase has latent potential to retain specificity while reacquiring some of the catalytic activity that was lost on removal of a large segment of protein.

We demonstrated direct selection of a mutant fragment with enhanced catalytic activity. This was done without knowledge of the three-dimensional structure of the protein. The idea is that, for any strain construction in which the cell growth rate is severely retarded because of limited activity of the enzyme of interest, a mutant enzyme with enhanced specific activity will have accelerated growth and a clear selective advantage.

Mutagenesis and selection were applied to a catalytic fragment of *Escherichia coli* alanine tRNA synthetase. The enzyme catalyzes a two-step aminoacylation reaction of $tRNA^{Ala}$. The first reaction is synthesis of aminoacyl adenylate, which can occur in the absence of $tRNA^{Ala}$. The second reaction is between the enzyme-bound adenylate and $tRNA^{Ala}$, to yield Ala-$tRNA^{Ala}$. The sum of the two reactions is the aminoacylation reaction.

The full-length enzyme is an 875–amino acid polypeptide (*5*). Aminoacylation of $tRNA^{Ala}$ requires a 461–amino acid $NH_2$-terminal fragment, as judged by an in vivo complementation assay (*3, 4*). Although the activity is sufficient to achieve complementation of a specific mutation in vivo, the aminoacylation activity in vitro is virtually undetectable. There is no evidence for activity in vivo or in vitro for an amino-terminal fragment having 76 fewer amino acids (fragment of 385 *alaS* amino acids).

The original plasmid construction that encodes the 461 $NH_2$-terminal *alaS* codons specifies a polypeptide that complements the temperature-sensitive *alaS5* mutation but does not complement a strain that carries the Δ*alaS2* null allele (*3, 4*). This suggests that improving the specific activity of the fragment in vivo could result in complementation of the null allele background.

Plasmids pMJ385Nt and pCH461Nt, respectively, encode the 385– and 461–amino acid fragments at the $NH_2$-terminal of alanyl-tRNA synthetase, plus a COOH-terminal "tail" of 14 codons derived from pBR322. Plasmid pCH461Nt complements (at 42°C) the temperature-sensitive *alaS5* mutation (*3*). Plasmid pMJ385Nt complements neither *alaS5* nor Δ*alaS2* mutant alleles. The polypeptide encoded by pCH461Nt has low aminoacylation activity (see below). Although it is sufficient to complement the *alaS5* strain, it is insufficient for complementation of a specially constructed null allele, Δ*alaS2* (*4, 6*).

Heteroduplexes between these plasmids were formed and subjected to bisulfite mutagenesis (*7, 8*) (Fig. 1). (Except for the deleted nucleotides in pMJ385Nt and a removed Sal I site in pCH461Nt, the two plasmids are identical.) The mutagenized DNA was passed through a *ung*$^-$ *alaS5* strain (*9*). This strain is temperature sensitive by virtue of the *alaS5* mutation; the uracil-*N*-glycosidase deficiency (*ung*$^-$) assures that mutant uracils are not excised. The *ung*$^-$ *alaS5* cells were also transformed with an untreated mixture of heteroduplex and linear DNA's. In this control experiment, about half of the transformants selected for plasmid-mediated ampicillin resistance ($Amp^r$) at the permissive temperature (30°C) were viable at the restrictive temperature (42°C). This established that segregation of the plasmids within the heteroduplex occurs after replication and that the deletion loop is retained in the 42°C transformants, because exci-

sion of this loop would prohibit complementation of the temperature-sensitive *alaS5* mutation.

The *ung*$^-$ *alaS5* cells transformed with NaCl- and bisulfite-treated DNA's gave two species of plasmids that were isolated from the pooled progeny arising at the permissive temperature. Both comigrated with the original plasmids. Digestion with Sal I preferentially linearized the smaller plasmid, as anticipated. (This allows pCH461Nt to be preferentially transformed because linear DNA transforms poorly.) The Sal I–digested pool of mutagenized DNA was then transformed into a Δ*alaS2*/pMJ901 strain to select for the desired mutant alanyl-tRNA synthetase fragments.

The Δ*alaS2* mutation is a null allele of *alaS* (*10*). Because *alaS* is an essential gene, this strain is maintained prior to transformation by an *alaS* plasmid (pMJ901), which also encodes tetracycline resistance (Tet$^r$) and has a temperature-sensitive origin of replication. In transformants harboring both pCH461Nt and pMJ901, the latter is selectively eliminated by shifting the temperature to 42°C (*10*).

For NaCl-treated DNA controls, no transformants arose at 42°C. This is consistent with the inability of pCH461Nt to complement Δ*alaS2* and indicates that prolonged exposure to high salt concentration has no enhancing mutagenic effects.

Heteroduplexes were treated with 4*M* bisulfite for 15, 60, 120, and 240 minutes. Viable colonies were observed at the restrictive temperature from cells transformed with each of the bisulfite-treated DNA samples. Of the Δ*alaS2* transformants that arose under permissive conditions, between 1 and 4 percent were viable at the higher temperature, where replication of the maintaining plasmid is blocked. The optimal number of mutant phenotypes was obtained with DNA that had been treated for 60 or 120 minutes with 4*M* bisulfite.

Mutations with deleterious effects were scored by the loss of complementation of the temperature-sensitive *alaS5* strain. With extensively mutagenized DNA (4 hours with 4*M* bisulfite), fewer than 3 percent of the *alaS5* transformants arising at 30°C were viable at 42°C. This indicates that large numbers of deleterious mutations had occurred. In contrast, equal numbers were viable at both temperatures for cells transformed with NaCl-treated DNA (see above).

The Δ*alaS2* transformants that were viable at 42°C were judged not to arise by reversion of the defective replication origin in pMJ901 because that plasmid's Tet$^r$ marker was lost at 42°C. That activity is borne by mutant pCH461Nt was shown when plasmid DNA from several viable colonies was back-transformed into the same strain and yielded transformants at a high frequency ($5 \times 10^4$ per microgram of DNA) at the restrictive temperature. We picked colonies with mutant phenotypes resulting from transformation with DNA that had been treated with bisulfite. To determine the locations of point mutations, a 0.8-kb Bgl II–Eco RI segment that spans the deletion loop (Fig. 1) was excised from mutant plasmids that complement Δ*alaS2*. This fragment was cloned into M13mp9 and sequenced by the dideoxy chain termination method (*11*). The orientation of the cloned segment was such that synthesis of the complementary chain extended from the Eco RI site—at the 3′ end of the truncated *alaS* coding strand—into the internal coding sequences for the fragment. In this direction, a single primer extension reaction was sufficient to determine the sequence of the entire deletion loop.

A summary of the point mutations found in seven different mutants is given in Table 1. Six of these have a mutation of glutamine to amber (CAG to TAG) at the codon following amino acid 461. This mutation precisely terminates the short extraneous segment of 14 codons derived from pBR322 sequences that are in-frame with the COOH-terminal end of pCH461Nt. One mutant (M0) has the nonsense mutation as the sole non-silent mutation, and it thus encodes the wild-type 461–amino acid $NH_2$-terminal fragment of alanine-tRNA synthetase. That M0 complements *alaS2* implies that removal of the tail enhances the activity in vivo.

Five of the mutants have the same amber mutation and one or more missense mutations. Two of them have one missense mutation, which is either $Ala_{394} \rightarrow Val$ (M1) or $Ala_{409} \rightarrow Val$ (M2). The three that have more than one missense change each have at least one of these mutations. A mutant (M6) that does not terminate after codon 461 was also scored. It has the string of 14 codons derived from pBR322. This has three mutations in the *alaS* coding section and none of these is found in any of the other mutants. It was not investigated further.

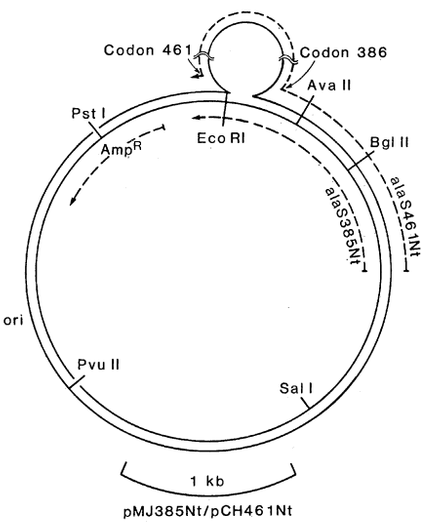


Fig. 1. Heteroduplex construction formed from plasmids pMJ385Nt and pCH461Nt. *Pvu*II-linearized pMJ385Nt (inner strand) and *Pst*I-linearized pCH461Nt (outer strand) were denatured and reannealed to form the plasmid heteroduplex shown. The single-stranded deletion loop contains codons 386 to 461 of *alaS*. Treatment with sodium bisulfite promotes deamination of cytosine to uracil within this region. Additional products from heteroduplexing that are not shown include reannealed linears and the complementary heteroduplex. The *alaS* temperature-sensitive *E. coli* strain KL380 (relevant genotype, *alaS5*) was provided by K. B. Low (*25*). The *alaS* chromosomal deletion mutant strain KL385 *recA*Δ1 Kan$^r$ A*alaS* was constructed as described by Jasin and Schimmel (*10*). BD1528-3a (relevant genotype, *ung-1 recA1 alaS5*) is a uracil *N*-glycosylase defective strain used to stably incorporate mutant uracils as thymines after bisulfite mutagenesis (*9*). The construction of plasmids pMJ385Nt and pMJ461Nt, which encode $NH_2$-terminal alanyl-tRNA synthetase fragment, is detailed elsewhere (*4*). The unique Sal I site in pMJ461Nt was eliminated by linearizing with Sal I, filling the staggered ends of the linear DNA, and recircularizing with T4 DNA ligase. Amp$^r$ transformants were screened for loss of the *Sal* I site and one plasmid (pCH461Nt) was selected for heteroduplexing. Plasmid pMJ385Nt was digested with Pvu II, and pCH461Nt was digested with Pst I. Heteroduplexes were formed from 4 μg of each linear DNA by the method of Peden and Nathans (*7*), and bisulfite mutagenesis was carried out by the method of Shortle and Nathans (*26*) [see also (*8*)]. Incorporation of thymine for uracil in the mutant plasmids was accomplished by transforming 1 μg of bisulfite-treated DNA into the *ung*$^-$ *alaS5* strain BD1528-3a. After a 2.5-hour expression period at 30°C, the culture was spread on several Luria-Bertani Amp agar plates containing ampicillin (100 μg/ml), and colonies arising after 48 hours were pooled. DNA isolated from pooled strains were used to transform *alaS5* and Δ*alaS2 Escherichia coli* mutants in the selection procedure. Plasmid DNA was isolated by a modification of the procedure of Katz *et al.* (*27*) or by the rapid boil method (*28*). DNA fragments subjected to electrophoresis in 1 percent agarose were isolated by electroeluting the fragment from excised gel slices. Competent *E. coli* was prepared and transformed (*29*). DNA was sequenced by the dideoxy chain termination method (*11*) with the use of derivatives of M13 phage templates (*30*).

Mutants M0, M2, M3, M4, and M5 were checked for mutations outside the target region. Each was sequenced for 250 base pairs beyond the 5′ side of the boundary of the deletion loop. No additional mutations were found. This confirms that mutagenesis was limited to a specific segment.

The Ava II–Eco RI fragment that spans the deletion loop was excised from mutant plasmids M0, M2, M3, and M5. The analogous DNA segment was removed from the recipient vector pMJ385Nt and replaced with the mutant DNA fragment so as to reconstruct the truncated *alaS* gene coding for mutant polypeptide. The reconstructed mutant plasmids complement the Δ*alaS2* null allele and in every other respect are identical to the original mutant plasmids (data not shown). This confirms that the mutations given in Table 1 are solely responsible for the mutant phenotype.

In vivo synthesis of the fragment from pCH461Nt, of wild-type fragment from M0 (plasmid pCH461N), and one of the mutant fragments (M2) was studied in maxicells (*12, 13*). Plasmid-encoded proteins were selectively labeled with [$^{35}$S]-methionine, separated by sodium dodecyl sulfate (SDS)–polyacrylamide gel electrophoresis and visualized by autoradiography (Fig. 2). The perceptible greater mobility of wild-type and $Val_{409}$ mutant fragments, as compared with that of the fragment from pCH461Nt, suggests that the modified polypeptides expressed in vivo lack the extraneous COOH-terminal amino acids, as expected. The similar intensities of the polypeptide bands suggest that the three fragments are stably synthesized and that their levels of expression are similar.

In vitro, the aminoacylation activity of the polypeptide encoded by pCH461Nt, which has the tail of 14 codons derived from pBR322, is so low that it is difficult to quantitate reliably. However, the alanine-dependent adenosine triphosphate–inorganic pyrophosphate (ATP-$PP_i$) exchange activity of this fragment appears unaltered from that of the full-length native enzyme.

We focused primarily on wild-type fragment M0, the two missense substitution mutants M1 and M2, and the double mutant M3. The initial analysis was done with crude extracts. As an internal standard, we checked the valine-specific aminoacylation activity because this should be the same for each extract. We established that each one had valine-specific aminoacylation activity within 20 percent of that of the extract for M0. The four extracts had the same (±10 percent) alanine-dependent ATP-$PP_i$ exchange specific activity (adenylate synthesis), suggesting that the adenylate synthesis domain is not disturbed in the mutants. This is consistent with other data showing that full alanine-dependent ATP-$PP_i$ exchange activity (equal to that of the full-length enzyme) is accomplished by the 385 $NH_2$-terminal amino acids, which are outside the region that was mutagenized (*4, 14*). The similar alanyladenylate synthesis activity of the various extracts also implies a similar protein concentration. The results of expression of M0 and M2 in maxicells corroborate this point.

Aminoacylation activity of wild-type fragment M0, in contrast to that of the polypeptide encoded by pCH461Nt, is easily detected. This is consistent with M0's complementation of the Δ*alaS2* allele and with the lack of complementation of this allele by pCH461Nt.

The alanine-dependent aminoacylation activity of the four extracts was investigated. For the wild-type fragment the aminoacylation specific activity is about 0.1 percent of that of full-length native alanine tRNA synthetase. We detected no difference in the normalized aminoacylation activity for the $Ala_{394}$ → Val mutant M1 when compared with that of the wild-type enzyme M0. Mutants M2 and M3, which have the $Ala_{409}$ → Val substitution either alone (M2) or combined with the $Ala_{394}$ → Val change (M3), have similar aminoacylation specific activities that are severalfold above that of wild-type fragment M0. (Quantitative values are given below.) We therefore investigated further the properties of the single substitution mutant M2.

The effect of the $Ala_{409}$ → Val mutation on catalytic activity was explored by measuring steady-state kinetic parameters for the $Ala_{409}$ → Val and wild-type fragments. Both fragments were purified to near homogeneity in a four-step procedure. In the ATP-$PP_i$ exchange reaction (*14*), the two fragments have nearly identical Michaelis constants ($K_m$'s) for alanine and ATP. The $K_m$ for alanine was measured by varying the amino acid from 0.1 to 2 m*M* at 2 m*M* ATP. The $K_m$ for ATP was determined by varying the nucleotide from 10 to 200 μ*M* at 5 m*M* alanine. For the wild-type fragment, these $K_m$'s are 0.7 m*M* (alanine) and 23 μ*M* (ATP) at *p*H 7.5 and 30°C; the mutant M2 parameters are 0.5 m*M* and 21 μ*M*, respectively. The same ATP-$PP_i$ exchange activity of the two fragments is not due, therefore, to compensating changes in the kinetic parameters. The sites for ATP and alanine appear undisturbed.

The difference in specific aminoacylation activity of wild-type and mutant enzyme extracts was corroborated with

Table 1. Amino acid substitutions in mutants that arise in the selection for higher catalytic activity. Mutants M0 to M5 arise from C → T transitions in the coding strand of the DNA, and mutant M6 arises from C → T transitions in the opposite strand. In addition to the missense mutations, some of the mutant genes also contained silent changes. The number of silent changes is M0, none; M1, two; M2, one; M3, one; M4, three, M5, two; and M6, none.

| Mutant | substitution |
|---|---|
| M0* | |
| M1† | $Ala_{394}$ → Val |
| M2† | $Ala_{409}$ → Val |
| M3† | $Ala_{394}$ → Val, $Ala_{409}$ → Val |
| M4† | $Ala_{394}$ → Val, $Ala_{443}$ → Val, $Ala_{454}$ → Val |
| M5† | $Ala_{409}$ → Val, $Arg_{415}$ → Cys |
| M6‡ | $Val_{405}$ → Ile, $Val_{419}$ → Ile, $Glu_{430}$ → Lys |

*Mutant M0 arises from a single base change in pCH461Nt. This change (CAG−>TAG) generates a stop codon immediately after codon 461 of *alaS*. This stops translation of the 14 codons derived from pBR322 which are fused to *alaS* in pCH461Nt. †Contains an amber stop codon after codon 461. This is generated by the same C → T transition as occurs in M0. ‡Contains a "tail" of 14 codons after *alaS* codon 461. These codons are derived from pBR322.

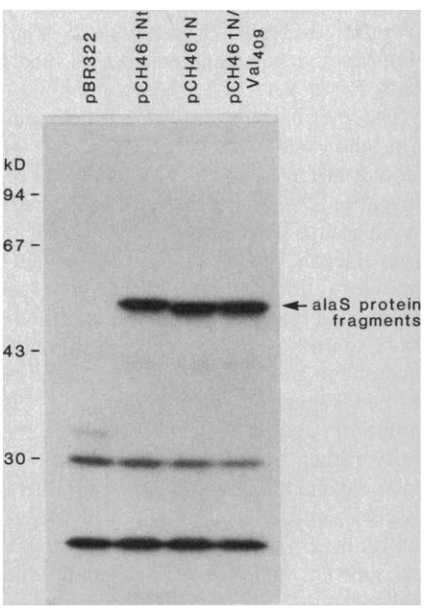


Fig. 2. Autoradiogram of a 10 percent SDS–polyacrylamide gel showing plasmid-encoded proteins selectively labeled with [$^{35}$S]methionine and expressed in transformed maxicells. Positions of molecular weight standards are indicated. The bottom band corresponds with the dye front. Plasmid-encoded proteins were selectively labeled with [$^{35}$S]methionine by the maxicell technique (*12*) and visualized on the 10 percent SDS–polyacrylamide gels (*31*) by autoradiography.

the purified enzyme. Differences in $k_{cat}/K_m$ ($k_{cat}$ is the catalytic constant) for tRNA in the aminoacylation reaction were observed from the dependence of initial velocity on the concentration of tRNA. In contrast to the native full-length alanyl-tRNA synthetase, which is at maximum velocity ($V_{max}$) with respect to tRNA in the range assayed (3.4 to 84 $\mu M$; $K_m$ [$tRNA^{Ala}$] = 0.6 $\mu M$), the rate of aminoacylation for the $Ala_{409} \rightarrow$ Val mutant was linear with tRNA up to [$tRNA^{Ala}$] = 40 $\mu M$, and that of the wild-type fragment was linear up to [$tRNA^{Ala}$] = 80 $\mu M$. (It is not feasible to do assays above 80 $\mu M$ $tRNA^{Ala}$ because of the amount of scarce material which is required and because of potential complications coming from tRNA aggregates, which may form at high concentrations.) The slope of the linear portion of the velocity versus ($tRNA^{Ala}$) plot is $k_{cat}/K_m$. For the $Ala_{409} \rightarrow$ Val mutant, this parameter is five times that of the wild-type fragment when purified $tRNA^{Ala}$ is used (Fig. 3). The magnitude of the $k_{cat}/K_m$ enchancement is similar whether measurements are made with purified protein or with cell extracts (not shown). Because of the excessively high $tRNA^{Ala}$ concentration required, we cannot further break down the individual components of $k_{cat}/K_m$.

The aminoacylation activity of the $Ala_{409} \rightarrow$ Val mutant fragment is unchanged whether unfractionated tRNA or purified $tRNA^{Ala}$ is acylated. This confirms that the fragment retains specificity for tRNA.

The thermal stability of purified mutant and wild-type fragments was assessed. No loss in activity was observed for either fragment at 30° and 37°C for up to 2.5 hours. With respect to the purification of each fragment, the ratio of alanine-dependent ATP-$PP_i$ activity to aminoacylation activity of the crude extract was not significantly different from that of the pure fragment. The findings further suggest that the $Ala_{409} \rightarrow$ Val mutation enhances intrinsic catalytic activity rather than fragment stability. A host strain with a Δ*alaS2* null allele (KL385 Δ*alaS2*) was maintained, separately, by a plasmid encoding full-length *alaS* protein, the wild-type fragment M0, and the mutant fragment M2. The doubling times in rich (Luria) broth at 37°C for the cells harboring fragments M0 and M2, and full-length native enzyme, are respectively, 100, 79, and 30 minutes. The faster growth rate of M2 may be related to the higher intrinsic enzyme activity of the mutant protein M2 in comparison with that of the wild-type fragment M0.

Polypeptide chain lengths of aminoacyl tRNA synthetases range from 300 to 1000 amino acids (*1, 2*). There are data supporting the concept of a modular arrangement of functional domains whereby additional polypeptide sequences are fused to a catalytic core that itself may comprise only a few hundred amino acid residues (*3, 4, 15, 16*). These additional amino acid sequences may perform other functions such as gene regulation (*17, 18*) or the synthesis of adenosine tetraphosphate adenosine, a pleiotropic regulatory molecule (*19–21*).

Strong selective pressure to retain these sequences may result from their being functionally integrated with the catalytic core to the point that they have

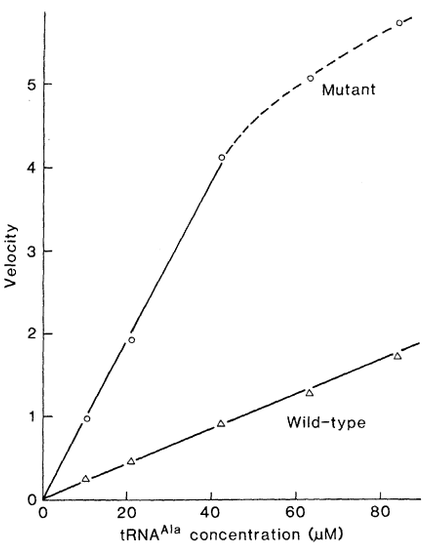


Fig. 3. Aminoacylation of $tRNA^{Ala}$ by wild-type and mutant $NH_2$-terminal fragments of alanyl-tRNA synthetase at *p*H 7.5 and 30°C. Reaction mixtures contained 8 $\mu M$ [$^3$H]alanine, 2 m$M$ ATP, and variable amounts of purified $tRNA^{Ala}$. The aminoacylation rates are reduced by the subsaturating concentrations of amino acid. To raise [$^3$H]alanine to saturating concentrations (over 1$M$) requires impractical amounts of radioactive substrate; the $K_m$ for alanine is identical, however, for the two fragments (see text). On the ordinate, velocity is measured as picomoles of alanyl $tRNA^{Ala}$ per picomoles of enzyme per minute. The slopes of the linear portions of these curves are $k_{cat}/K_m = 350M^{-1}$ $sec^{-1}$ (wild type) and $1700M^{-1}$ $sec^{-1}$ (mutant). The $NH_2$-terminal fragment of alanyl-tRNA synthetase was purified in four steps that included cell lysis, DEAE-cellulose chromatography, uridine 2′,5′- and 3′,5′-diphosphate agarose (UDP-agarose) affinity chromatography, and gel filtration (*32*). The purified fragments are at least 80 percent pure, as judged by polyacrylamide gel electrophoresis, and comigrated at the anticipated molecular weight. The ratio of aminoacylation to ATP-PPi exchange activity remained approximately constant throughout the purification. The aminoacylation reaction was performed at 30°C by the method of Schreier and Schimmel (*33*) as modified by Starzyk *et al.* (*34*).

actual determinants for catalysis (for example, by providing part of the site for binding of tRNA) (*4, 22*). If the residual protein that is mutagenized in these studies is akin to the alanyl-tRNA synthetase progenitor, then the likelihood of success is greatly increased. By the same reasoning, large enzymes that evolve from small progenitors might themselves be amenable to the type of reconstruction demonstrated here.

We believed it might be possible to select enhanced activity mutants of 461Nt that are in the *alaS* coding sequence, without removal of the 14-codon PBR322 portion. The selection repeatedly yielded the glutamine-to-amber codon change immediately after codon 461. This in itself was sufficient to increase activity over that of 461Nt. The Δ*alaS2* strain nonetheless grows quite slowly (see above) when the plasmid that is introduced contains just this mutation. Improved growth is seen with a plasmid that also has the $Ala_{409} \rightarrow$ Val substitution, and this single change gives a further increase in activity. It appears, therefore, that the selection goes beyond just that for acquiring the glutamine-to-amber mutation.

We obtained one mutant (M6) without the glutamine-to-amber change and with three missense mutations in the *alaS* coding sequence (Table 1). The specific aminoacylation activity of M6 in extracts is higher than that of M0 and is comparable to that of the $Ala_{409} \rightarrow$ Val mutant (*23*). This further suggests that activity levels higher than those of mutant M0 are obtained by the selection. It also suggests that a number of routes are available to achieve higher specific activity and that the effects of the 14-codon tail can be more than compensated for by mutations within *alaS* itself.

We estimate that the activity of the wild-type fragment M0 is several times that of the enzyme encoded by pCH461Nt. Since mutant M2 (and presumably M6) has activity five times that of M0, we conclude that the selection can yield mutant proteins with activities at least an order of magnitude higher than that of the starting polypeptide.

The faster doubling time of Δ*alaS2* strains expressing the $Ala_{409} \rightarrow$ Val fragment indicates that the $Ala_{409} \rightarrow$ Val replacement confers a selective growth advantage. The elevated $k_{cat}/K_m$ is a likely contributing factor. Intracellular concentrations of each tRNA species have been estimated at approximately 1 $\mu M$ (*24*). At these levels of tRNA, both mutant and wild-type fragments, having high $K_m$'s for tRNA, would operate under conditions in which activity is governed

by $k_{cat}/K_m$. Thus, any elevation in this parameter increases steady-state aminoacylation, accordingly improving growth under conditions in which the acylation of $tRNA^{Ala}$ is likely to be growth-limiting.

Our results suggest that when cell growth is limited or prevented by a specific catalytic activity, it is possible to select mutant forms of a catalytic unit having a higher intrinsic activity. The relative ease with which mutants were obtained, with a single mutagen that is restricted to G-to-A and C-to-T transitions, suggests that many more enhanced activity mutants could be selected by saturating the system with other mutagens.

### References and Notes


1. J. Ofengand, in *Molecular Mechanisms of Protein Biosynthesis*, H. Weissbach and S. Peska, Eds. (Academic Press, New York, 1977), pp. 7–69.
2. P. R. Schimmel and D. Soll, *Annu. Rev. Biochem.* **48**, 601 (1979).
3. M. Jasin, L. Regan, P. Schimmel, *Nature (London)* **306**, 441 (1983).
4. ———, *Cell* **36**, 1089 (1984).
5. S. D. Putney *et al.*, *Science* **213**, 1497 (1981).
6. M. Jasin, thesis, Massachusetts Institute of Technology (1984).
7. K. W. C. Peden and D. Nathans, *Proc. Natl. Acad. Sci. U.S.A.* **79**, 7214 (1982).
8. M. Jasin and P. Schimmel, *Gene Expression, Alfred Benzon Symposium 19*, B. F. C. Clark and H. U. Petersen, Eds. (Munksgaard, Copenhagen, 1984), pp. 223–235.
9. B. K. Duncan, P. A. Rockstroh, H. R. Warner, *J. Bacteriol.* **134**, 1039 (1978).
10. M. Jasin and P. Schimmel, *ibid.* **159**, 783 (1984).
11. F. Sanger, S. Nicklen, A. R. Coulson, *Proc. Natl. Acad. Sci. U.S.A.* **74**, 5463 (1977).
12. A. Sancar, A. M. Hack, W. D. Rupp, *J. Bacteriol.* **137**, 692 (1979).
13. T. Keng, T. A. Webster, R. T. Sauer, P. Schimmel, *J. Biol. Chem.* **257**, 12503 (1982).
14. S. D. Putney, R. T. Sauer, P. R. Schimmel, *ibid.* **256**, 198 (1981).
15. T. Webster *et al.*, *Science* **226**, 1315 (1984).
16. P. Schimmel, M. Jasin, L. Regan, *Fed. Proc. Fed. Am. Soc. Exp. Biol.* **43**, 2987 (1984).
17. S. D. Putney and P. R. Schimmel, *Nature (London)* **291**, 632 (1981).
18. P. Lestienne, J. A. Plumbridge, M. Grunberg-Manago, S. J. Blanquet, *J. Biol. Chem.* **259**, 5232 (1984).
19. E. Rapaport, P. C. Zamecnik, E. F. Baril, *Proc. Natl. Acad. Sci. U.S.A.* **78**, 838 (1981).
20. A. Varshavsky, *Cell* **34**, 711 (1983).
21. P. C. Lee, B. R. Bochner, B. N. Ames, *J. Biol. Chem.* **258**, 6827 (1983).
22. M. Jasin, L. Regan, P. Schimmel, *ibid.* **260**, 2226 (1985).
23. C. Ho, unpublished results.
24. J. A. Lewis and B. N. Ames, *J. Mol. Biol.* **66**, 131 (1972).
25. G. Theall, K. B. Low, D. Soll, *Mol. Gen. Genet.* **156**, 221 (1977).
26. D. Shortle and D. Nathans, *Proc. Natl. Acad. Sci. U.S.A.* **75**, 2170 (1978).
27. I. Katz, D. T. Kingsbury, D. R. Helinski, *J. Bacteriol.* **132**, 349 (1973).
28. D. S. Holmes and M. Quigley, *Anal. Biochem.* **114**, 193 (1981).
29. D. A. Morrison, *J. Bacteriol.* **132**, 349 (1977).
30. J. Messing, R. Crea, P. H. Seeburg, *Nucleic Acids Res.* **9**, 309 (1981).
31. U. K. Laemmil, *Nature (London)* **227**, 680 (1970).
32. J. Bowie and P. Schimmel, unpublished results.
33. A. A. Schreier and P. R. Schimmel, *Biochemistry* **11**, 1582 (1972).
34. R. M. Starzyk, S. W. Koontz, P. R. Schimmel, *Nature (London)* **298**, 136 (1982).

35. C.H. is currently at Division of Biology, California Institute of Technology, and M.J. is at Institut für Molekularbiologie II, der Universität Zürich, Switzerland. Supported in part by W. R. Grace & Co.

8 February 1985; accepted 22 May 1985

# Molecular Cloning of a Gene Sequence Regulated by Nerve Growth Factor

Abstract. *Nerve growth factor (NGF) is essential for the development and differentiation of sympathetic or sensory neurons. A complementary DNA was cloned that corresponds to a gene sequence induced more than 50-fold in a cultured target cell line of pheochromocytoma cells (PC12 cells) 5 hours after the addition of NGF. The induced messenger RNA encodes a 90,000-dalton polypeptide that may represent one of the primary events in NGF-induced differentiation of neurons.*

ANDREA LEVI*
JUANITA D. ELDRIDGE
BRUCE M. PATERSON
*Laboratory of Biochemistry, National Cancer Institute, National Institutes of Health, Bethesda, Maryland 20205*

*On leave of absence from Istituto di Biologia Cellulare, Via Romagnosi 18/A, Rome, Italy.

Nerve growth factor (NGF) is required for the development and maintenance of sympathetic and sensory neurons both in vivo and in vitro (*1*, *2*). In addition, it induces the differentiation of immature (*3*) and neoplastic chromaffin cells towards a neuronal phenotype, as exemplified by the PC12 cell line derived from a rat pheochromocytoma (*4*). While numerous biochemical effects of NGF on PC12 cells have been described, it has been difficult to correlate any of these effects with the induction of the neuronal phenotype. Even though induction of the neuronal phenotype requires RNA synthesis (*5*), Garrels and Schubert (*6*) and McGuire and Greene (*7*) reported no qualitative change in the protein pattern during induction in two-dimensional gel analyses of more than 800 proteins in PC12 cells. These authors suggested that NGF produced only quantitative modulations of protein synthesis rather than a qualitative change in the pattern of gene expression. We have investigated NGF modulation of gene expression in PC12 cells by identifying messenger RNA's (mRNA's) induced within 24 hours after exposure to NGF, a period that is 48 to 72 hours prior to the appearance of major morphological changes.

A complementary DNA (cDNA) library of approximately 5000 clones was constructed as described in the legend to Fig. 1 with mRNA isolated from PC12 cultures that had been treated with 2.5*S* NGF (100 ng/ml) for 24 hours (*8*). Those cDNA clones that gave a stronger hybridization signal with total cDNA probe from induced as compared to uninduced cells were selected and rescreened two additional times by the same procedure. Six clones were judged to represent NGF-induced RNA. This group of

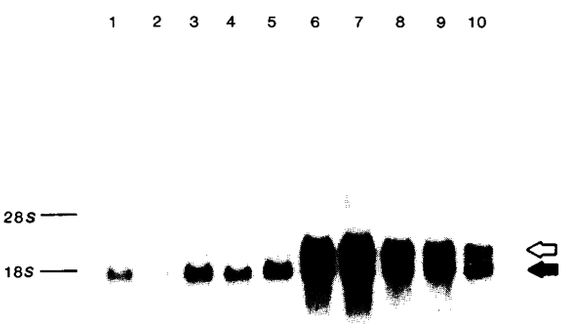


Fig. 1. Induction of the mRNA hybridizing to the VGF8a cDNA clone. Total RNA was prepared from cells treated as described (*16*). Approximately 10 μg of total RNA was subjected to electrophoresis in formaldehyde gels and blotted as described (*17*). The blot was hybridized with approximately $4 \times 10^6$ count/min per milliliter (10 ml) of the nick-translated VGF8a and rat actin cDNA clones. Equal amounts of plasmid DNA were mixed prior to labeling to obtain probes of comparable specific activity during nick translation. Conditions for the hybridization were as described (*18*). The cDNA library was prepared from 28 μg of oligodeoxythymidylate [oligo(dT)]–selected RNA (*19*) extracted from PC12 cells that had been treated with 2.5*S* NGF (100 ng/ml) for 24 hours. Hind III and Eco RI linkers were added to the ends of the double-stranded cDNA corresponding to the 3′ and 5′ ends of the RNA's, respectively, as described (*20*). *Escherichia coli* (DH1) were transformed with the recombinant DNA according to Hanahan (*21*). (Lane 1) RNA from FTRL5 cells; (lane 2) RNA from FTRL5 cells treated for 24 hours with 2.5*S* NGF (200 ng/ml); (lane 3) RNA from $GH_3$ cells; (lane 4) RNA from HTC cells; (lanes 5 to 10) RNA from PC12 cells treated with NGF (250 ng/ml) for 0, 3, 5, 9, 25, and 49 hours, respectively. The open arrow indicates the position of the RNA hybridizing with VGF8a cDNA clone. The solid arrow indicates the position of the actin RNA.